

# Research on Compensation of Solar Bracket Tracking Based on Error Model

Zhang Fan

Beijing Jiaotong University

Beijing, 100044, China

E-mail: zhangfanvo@163.com

**Abstract**—In recent years, photo voltaic industry has achieved rapid development, and the investment in large-scale photo voltaic power plants has eased the supply of electricity in more information-poor regions. There are intelligent control methods in high-power solar power systems where solar position tracking technology and plays an vital role. Based on the sun position tracking technology, the tracking error model in the sun positioning is established to analyze the error precision of the tracking algorithm, and the algorithm compensation factor is optimized to obtain the best positioning tracking effect in this paper. Moreover, the research on the compensation analysis of the photo voltaic tracking bracket error provides a guarantee for the power generation efficiency of the photo voltaic power station.

**Keywords**-Solar Bracket; Error Model; Tracking Compensation

## I. INTRODUCTION

Photovoltaic power generation system where advantages such as high power generation efficiency, small production pollution and high land utilization rate exists is composed of power generation module, tracking bracket, inverter boosting and communication monitoring, which has attracted more and more attention. The two-axis tracking bracket is composed of a column, a grid, a rotating mechanism in the horizontal as well as vertical directions, and a tracking controller. Besides it, solar module is mounted on the grid, and the position of the sun which horizontal and pitch rotation mechanism drives the solar module to rotate to in horizontal and pitch direction under the control and driving of the tracking controller is decomposed into two angles of horizontal and vertical, and the position needs to be aligned. In the case of solar motion, the bracket also follows its motion and remains in the right direction so that the sun shines perpendicularly on the module surface. Additionally, the characteristics of photovoltaic power generation require tracking brackets to accurately track the sun[1-3].

Nowadays, there are time control where astronomical algorithm is used to calculate and track the sun position according to the geographical location and time of the support, light control where the position of the sun is sensed through the light sensor, and the bracket tracks the sun and maximum power point search which is to search for the maximum power generated by the module through the power detecting component, and use the position where the

maximum power appears as the position facing the sun three kinds of ways to track the control mode of the bracket. Moreover, time control method is simple to implement, but it is affected by the mounting error of the bracket. Even if the sun position is calculated accurately, there will be tracking error. As for light control mode, although it is accurate in the case of good sunlight, it is vulnerable to cloud layer so that tracking blind zone will occur. When it comes to maximum power search mode which achieves maximum power output while there is power loss during the search, it needs to be corrected frequently[4-6]. Since time-controlled tracking cannot be used alone due to the large impact of installation, at present, light control is combined with time control or time control is combined with maximum power search in actual engineering, where time tracking is used for rough tracking, and the sun is controlled by light control or maximum power search. Analysis and research method of feedforward inverse compensation control is proposed in this paper to study the photovoltaic support and try to solve the problem that the tracking accuracy of the support is affected by the installation accuracy.

## II. SOLAR BRACKET TRACKING MODELING

The initial attitude of the solar bracket grid is vertically downward facing south, then the horizontal direction is selected as the reference coordinate system  $x_0$ , and the pitch direction is selected vertically as the reference coordinate system  $z_0$ . The rotation direction conforms to the left-hand rule, and  $x$  coordinate represents the normal of the module face on the grid[7].

### A. Principle of Coordinate Tracking

For a chasing process starting from the reference coordinate system, it can be broken down into the following steps.

1) The horizontal direction starts from  $x_0$  by rotating  $\lambda_1$  to  $x_1$  around the  $z_0$  axis, and  $z_0$  is rotated by  $90^\circ$  to  $z_1$  around  $x_1$ .

2)  $x_1$  rotates  $\lambda_2$  to  $\lambda_2$  around the  $\lambda_2$  axis, where  $z_2$  coincides with  $z_1$ .

After the process, the normal  $x_2$  of the module face which faces the sunpoints to the direction of the sun.

D-H parameters is shown in Table 1.

**TABLE I. D-H NOTATION PARAMETER TABLE WITHOUT INSTALLATION ERROR**

joint	$\lambda / ^\circ$	d/m	a/m	$\mu / ^\circ$
2	$\lambda_2$	0	0	0
1	$\lambda_1$	0	0	90

Coordinate transformation homogeneous square matrix is as follows.

$$\begin{bmatrix} C\lambda_1 & 0 & S\lambda_1 & 0 \\ S\lambda_1 & 0 & -C\lambda_1 & 0 \\ 0 & 1 & 0 & 0 \\ 0 & 0 & 0 & 1 \end{bmatrix} \times \begin{bmatrix} C\lambda_2 & -S\lambda_2 & 0 & 0 \\ S\lambda_2 & C\lambda_2 & -C\lambda_1 & 0 \\ 0 & 0 & 1 & 0 \\ 0 & 0 & 0 & 1 \end{bmatrix} \times \begin{bmatrix} 1 \\ 0 \\ 0 \\ 0 \end{bmatrix} = \begin{bmatrix} C\lambda_1 S\lambda_2 \\ S\lambda_1 C\lambda_2 \\ S\lambda_2 \\ 0 \end{bmatrix} \quad (1)$$

In equation (1),  $\lambda_1$  is the horizontal rotation angle (positive south is the starting 0°), and  $\lambda_2$  refers to the pitch rotation angle (the level is the starting 0°).

In addition, for the convenience of writing,  $S\lambda_1$  represents the sine of  $\lambda_1$ , and  $C\lambda_2$  indicates the cosine of  $\lambda_2$ .

$$\begin{bmatrix} C\lambda_1 & -S\lambda_1 C\eta_1 & S\lambda_1 S\eta_1 & 0 \\ S\lambda_1 & C\lambda_1 C\eta_1 & -C\lambda_1 S\eta_1 & 0 \\ 0 & S\lambda_1 & C\eta_1 & 0 \\ 0 & 0 & 0 & 1 \end{bmatrix} \times \begin{bmatrix} C\lambda_2 & -S\lambda_2 & 0 & 0 \\ S\lambda_2 & C\lambda_2 & 0 & 0 \\ 0 & 0 & 1 & 0 \\ 0 & 0 & 0 & 1 \end{bmatrix} \times \begin{bmatrix} 1 \\ 0 \\ 0 \\ 0 \end{bmatrix} = \begin{bmatrix} C\lambda_1 C\lambda_2 - S\lambda_1 C\eta_1 S\lambda_2 \\ S\lambda_1 C\lambda_2 + C\lambda_1 C\eta_1 S\lambda_2 \\ S\eta_1 S\lambda_2 \\ 0 \end{bmatrix} \quad (2)$$

In formula (2),  $\eta_1$  is the angle between the beam and the horizontal direction.

### III. ERROR ANALYSIS

Effectively eliminating parameter errors has become one of the key technologies for tracking bracket accuracy control. First, tracking error caused by the beam installation error is analyzed with specific examples. The latitude and longitude of the test point obtained by GPS is east longitude 113°26'11" north latitude 22°33'49". At 12:10:00 am on July 11, 2019, Beijing time (East 8 District), the height and azimuth of the sun are  $h = 84.96^\circ$  and  $\eta = -85.62^\circ$ . Assuming that 1~89° is caused by the installation error of -1, if the solar elevation angle and azimuth angle are directly used as the control amount of the bracket, that is,  $\lambda_1 = -85.62^\circ$  and  $\lambda_2 = 84.96^\circ$ , the data are brought into the ideal conditions and the normal coordinates with error condition as well as the equations (1) and (2). What is respectively obtained is as follows[10].

### B. Modeling of Bracket Motion with Installation Deviation of Grid Beam

The bracket will be biased in three aspects during the installation. The column should be installed vertically, but the actual installation will not be completely vertical, which will result in two errors in deviation direction and deviation amount. What's more, horizontal installation which is not completely horizontal is required in grid, then installation deviation that is regarded as the degree of freedom of bracket modeling will appear. The following is an example of the horizontal deviation of the grid, and the modeling is shown in Table 2[8-9].

**TABLE II. D-H NOTATION PARAMETER TABLE WITH INSTALLATION ERROR**

joint	$\lambda / ^\circ$	d/m	a/m	$\mu / ^\circ$
2	$\lambda_2$	0	0	0
1	$\lambda_1$	0	0	$\eta_1$

Coordinate transformation homogeneous square matrix is as follows.

$$\begin{bmatrix} C\lambda_1 C\lambda_2 \\ S\lambda_1 C\lambda_2 \\ S\lambda_2 \\ 0 \end{bmatrix} = \begin{bmatrix} 0.006709 \\ -0.087595 \\ 0.996134 \\ 0 \end{bmatrix} \quad (3)$$

$$\begin{bmatrix} C\lambda_1 C\lambda_2 - S\lambda_1 C\eta_1 S\lambda_2 \\ S\lambda_1 C\lambda_2 + C\lambda_1 C\eta_1 S\lambda_2 \\ S\eta_1 S\lambda_2 \\ 0 \end{bmatrix} = \begin{bmatrix} 0.024043 \\ -0.086267 \\ 0.095982 \\ 0 \end{bmatrix}$$

Azimuth and elevation angle corresponding to the normal vector are separately calculated as followed.

$$\begin{cases} \arctan\left(\frac{-0.087595}{0.006709}\right) = -85.62 \\ \arcsin(0.996134) = 84.96 \end{cases} \quad (4)$$

$$\begin{cases} \arctan\left(\frac{-0.086267}{0.024043}\right) = -74.43 \\ \arcsin(0.995982) = 84.86 \end{cases} \quad (5)$$

Azimuth tracking error at different installation errors at this time is obtained.

From the above analysis, the following conclusions can be drawn. Under ideal conditions, according to the astronomical algorithm the attitude angle of the module obtained by controlling the travel of the two axes is consistent with the angle calculated based on astronomical algorithm. Moreover, in the case of error, there is an error in

the attitude angle of the module obtained by the biaxial travel amount controlled by the astronomical algorithm, and the error may be very large at a certain time and angle. In the above example, a mounting error of only 1 results in a tracking error in azimuth  $(-74.43^\circ) - (-85.62^\circ) = 11.19^\circ$ . During the entire tracking process, the error varies in the range  $[0, \varpi_{\max}]$ , and  $\varpi_{\max}$  represents the maximum error.

#### IV. INVERSE MODEL SOLUTION IN DELAY COMPENSATION MECHANISM

##### A. Kinematics Model Analysis

Kinematic model equation of tracking bracket is obtained from the previous positive kinematics analysis. The inverse kinematics solution will be solved by the equation below, and several useful formulas are derived.

It is hoped that in the presence of installation errors, the attitude of the bracket rotating under the control of height angle  $\lambda_2$  and azimuth  $\lambda_1$  is consistent with the attitude without error (ideal conditions), that is, the normal vector of the light-receiving surface in the module coincides with the vector of the sun light, which can be expressed as follows.

$$\begin{bmatrix} C\lambda_1 C\lambda_2 - S\lambda_1 C\eta_1 S\lambda_2 \\ S\lambda_1 C\lambda_2 + C\lambda_1 C\eta_1 S\lambda_2 \\ S\eta_1 S\lambda_2 \\ 0 \end{bmatrix} = \begin{bmatrix} CaCh \\ SaCh \\ Sh \\ 0 \end{bmatrix} \quad (6)$$

If the error angle  $\eta_1$  is known, the height angle and azimuth angle of the sunlight can be obtained by astronomical algorithm, then the control angles  $\lambda_2$  and  $\lambda_1$  of the bracket height and orientation can be solved by the following formula.

$$S\eta_1 S\lambda_2 = Sh, \lambda_2 = \arcsin\left(\frac{\sinh}{\sin\eta_1}\right) \quad (7)$$

From equation (7),  $\lambda_1$  and  $\lambda_2$  which refers to running angle of the bracket as well as the actual control angle of the bracket can be obtained. Under the control of  $\lambda_1$  and  $\lambda_2$ , the bracket can be aligned with the sun with the installation error to achieve the ideal control requirements, which is the inverse kinematic solution.

##### B. Error Compensation

From the previous derivation, the kinematic model of the mounting error in the bracket can be obtained, and according to the working range of the solar tracking bracket, the transfer function of the piezoelectric ceramic can be simplified into a first-order inertial system.

$$Tw(t) + w(t) = v(t) + \Delta \quad (8)$$

In equation (8)  $T$  is the time constant,  $v$  represents the input of the inverse model,  $w$  refers to the output of the inverse model, and  $\Delta$  indicates the disturbance. Assuming  $\Delta$

is bounded,  $|\Delta| \leq D$ ,  $D > 0$  is the upper bound of the disturbance.

$\lambda$  is used to instated of  $T$ , then equation (9) can be written as follows.

$$\lambda w(t) + w(t) = v(t) + \Delta \quad (9)$$

Systematic error can be defined as:

$$e = w_r - w_d \quad (10)$$

Define the function:

$$s = Ce \quad (11)$$

If  $C=1 > 0$  which satisfied the Hurwitz condition, there will be

$$\dot{s} = \dot{e} = \dot{w}_{dr} - \dot{w}_d \quad (12)$$

Equation (8) is substituted into equation (12), then

$$\dot{s} = \frac{1}{\lambda}(v - w_r) - \dot{w}_d \quad (13)$$

The control law can be designed as follows.

$$u_{smc} = u_a + u_{s1} + u_{s2} \quad (14)$$

The control law  $u_{smc}$  can be expressed as:

$$u_a = \hat{\lambda} w_d \quad (15)$$

$$u_{s1} = -k_s s \quad (16)$$

$$u_{s2} = -\eta s \operatorname{gn}(s) \quad (17)$$

In equation (17)  $u_a$  is the adaptive compensation term,  $\hat{\lambda}$  represents the adaptive estimate of  $\lambda$ ,  $u_{s1}$  refers to the feedback term, and  $u_{s2}$  is the robust term,  $k_s > 0$ ,  $\eta > D$ .

Lyapunov can be defined as

$$v = \frac{1}{2} \lambda s^2 + \frac{1}{2\gamma} \dot{\lambda}^2 \quad (18)$$

where  $\lambda' = \lambda'' - \lambda$ ,  $\gamma > 0$ , then

$$\dot{v} = \frac{1}{2} \dot{\lambda} s^2 + \frac{1}{2\gamma} \lambda' \lambda'' s^2 = s[(v - w_r) - \lambda \dot{w}_d \Delta] + \frac{1}{\gamma} \lambda' \lambda'' \quad (19)$$

If the adaptive law is

$$\hat{\lambda} = -\gamma \dot{w}_d s \tag{20}$$

then

$$\begin{aligned} \dot{V} &= s \dot{\lambda} \dot{x}_d - s[k_s s + \eta s \text{sgn}(s)] - \lambda \dot{x}_d s + \frac{1}{\gamma} \lambda' \lambda'' + \Delta_s = \\ \hat{\lambda} \dot{x}_d s - s[k_s s + \eta s \text{sgn}(s)] + \Delta_s &= \\ -k_s s^2 - \eta s \text{sgn}(s) s + Ds &< -k_s s^2 \leq 0 \end{aligned} \tag{21}$$

In order to reduce the impact of buffeting, the saturation function sat(s) takes place of the symbol function.

$$\text{sgn}(s) \begin{cases} 1 & s > h \\ ks & |s| \leq h, k = 1/h \\ -1 & s < -h \end{cases} \tag{22}$$

In equation (22)  $h$  is the boundary layer, and the nature of the saturation function is that switching control is used outside the boundary layer, while linearized feedback control is used in the boundary layer.

After replacing the symbol function with a saturation function, other cases are similar to the symbol function. When  $|s| \leq h$ , the value of  $\eta$  is required to be large enough. In summary, it is only necessary to take a larger  $\eta$  value to satisfy the negative derivative in Lyapunov function, that is, when time  $t \rightarrow \infty, s=0, e=0, \dot{e}=0$ , the designed control law can make the system globally stable.

## V. EXPERIMENTAL ANALYSIS

### A. Tracking Accuracy Experiment

According to the experimental input and output data,  $T=8, k_s=400, \gamma=30$  are selected. Moreover, system mentioned above is simulated by Simulink, and the result is shown in Fig. 1.

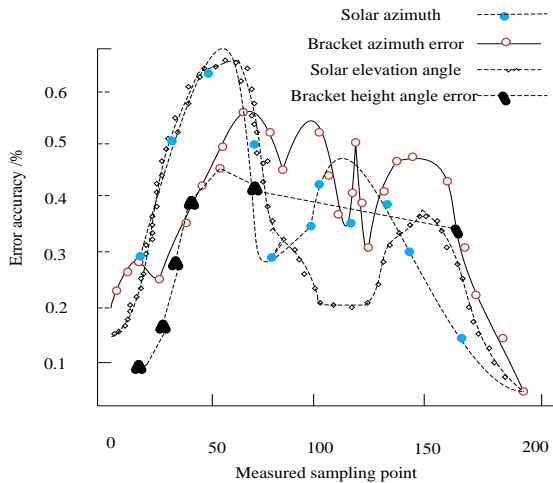


Figure 1. Measured error curve between height and azimuth of the bracket and the sun

In Fig. 1, the actual correlation data and test data are converted into tracking curve from which it can be clearly seen that the accuracy of the uncompensated tracking algorithm is not accurate enough, and the calculation deviations of the elevation and the azimuth angle are both larger than the sun running trajectory. The details of the tracking curve after 3s compensation are selected as shown in Fig. 2.

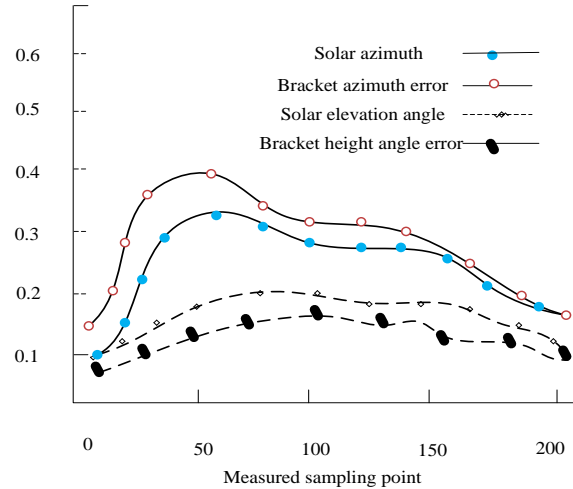


Figure 2. Tracking curve between the height and azimuth of the bracket after error compensation and the sun

It can be seen from the compensated curve that the tracking curve actually fluctuates up and down the ideal curve with an error of less than 4%, which indicates the effectiveness of the control algorithm. Meanwhile, it can also be seen from the above figure that the theoretical calculation effect of the compensated bracket is basically consistent with the actual tracking effect, and the two curves are basically coincident, which illustrates that the tracking accuracy can be achieved only with the help of time control after error compensation.

### B. Hysteresis Compensation Experiment

The feedforward and adaptive control are combined to perform the hysteresis compensation experiment according to the relationship between voltage and displacement 1:100. The voltage is changed every 10s, and the data is collected every 500ms, which is shown in Figure 3.

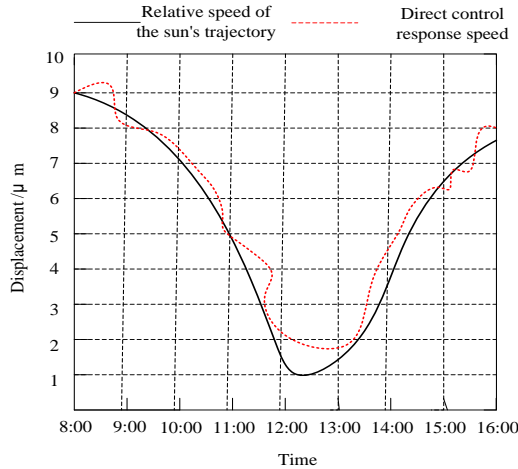


Figure 3. Tracking Displacement Response Speed Curve before Control

The dotted line in Fig. 3 is the displacement curve before the control, and the solid line refers to the displacement curve of the solar operation, which shows that the hysteresis characteristic before control is obvious, the same displacement is basically identical after the control, and hysteresis is suppressed. In order to reduce the measurement error, all the displacement measurements at the same voltage are averaged and the displacement curve is plotted, which is shown in Figure 4.

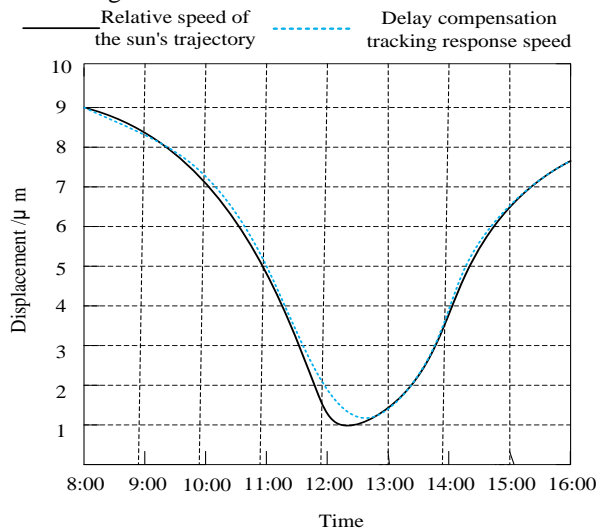


Figure 4. Delay Compensation Tracking Displacement Response Speed Curve

The maximum hysteresis before control is  $0.873\mu\text{m}$ , and it turns  $0.494\mu\text{m}$  after control, which is reduced by 48.1%. The hysteresis is effectively suppressed.

Feedforward inverse compensation control and adaptive direct control are used to track the same set of sinusoidal signals with different frequencies, and the obtained experimental data is collected and processed. Moreover, the

discrete point is the expected displacement point, solid line is the tracking error under direct control, and the point line is the tracking error under the feedforward inverse compensation control. In addition, the error decreases from  $2.37\mu\text{m}$  to  $1.27\mu\text{m}$ , which is decreased by 27%. Besides it, the average absolute error decreased from  $0.095\mu\text{m}$  to  $0.078\mu\text{m}$ , which is decreased by 17.9%. From the above data, it can be obtained that the inverse compensation control is more stable than the direct control.

## VI. CONCLUSION

In order to solve the problem that the time-controlled mode of the solar tracking bracket is not affected much by the installation, why track accuracy is affected by installation error compensated later is found by establishing the kinematics model of the tracking bracket, which improves the accuracy of time tracking and meets the tracking requirements on photovoltaic power generation.

## REFERENCES

- [1] GUO Qing, YIN Jingmin, YU Tian, et al. Saturated adaptive control of electrohydraulic actuator with parametric uncertainty and load disturbance[J]. IEEE Transactions on Industrial Electronics, 2017, PP(99): 1-1.
- [2] GUO Qing, ZHANG Yi, BRANKO G. Celler, et al. Backstepping Control of Electro-Hydraulic System Based on Extended-State-Observer with Plant Dynamics Largely Unknown[J]. IEEE Transactions on Industrial Electronics, 2016, 63(11): 6909-6920.
- [3] Song X, Duggen L, Lassen B, et al. Modeling and Identification of Hysteresis with Modified Preisach Model in Piezoelectric Actuator[C]//2017 IEEE International Conference on Advanced Intelligent Mechatronics (AIM). IEEE, 2017: 1538-1543.
- [4] Bermúdez A, Dupré L, Gómez D, et al. Electromagnetic Computed-Torque Technology for Transducers. seu.edu.cn Volume 32: Issues with Preisach Hysteresis Model[J]. Finite Elements in Analysis & Design, 2017, 126(4): 65-74.
- [5] Monnor T, Kanchiang K, Yimnirun R, et al. Modeling and Characterization of Hysteresis Loops with Preisach Hysteron Weight Modification[J]. Integrated Ferroelectrics, 2016, 175(1): 33-43.
- [6] Stefanski F, Minorowicz B, Persson J, et al. Non-Linear Control of a Hydraulic Piezo-Valve Using a Generalised Prandtl-Ishlinskii Hysteresis Model[J]. Mechanical Systems & Signal Processing, 2017, 82(1): 412-431.
- [7] Ma J, Tian L, Li Y, et al. Hysteresis Compensation of Piezoelectric Deformable Mirror Based on Prandtl-Ishlinskii Model[J]. Optics Communications, 2018, 416(6): 94-99.
- [8] Gan Minggang, Qiao Zhi, Li Yanlong. Sliding Mode Control with Perturbation Estimation and Hysteresis Compensator Based on Bouc-Wen Model in Tackling Fast-Varying Sinusoidal Position Control of a Piezoelectric Actuator[J]. Journal of Systems Science & Complexity, 2016, 29(2): 367-381.
- [9] Wang G, Chen G, Bai F. Modeling and Identification of Asymmetric Bouc-Wen Hysteresis for Piezoelectric Actuator via a Novel Differential Evolution Algorithm[J]. Sensors and Actuators A: Physical, 2015, 235(11): 105-118.
- [10] Kim J S, Kim G W. Hysteresis Compensation of Piezoresistive Carbon Nanotube / Polydimethylsiloxane Composite-Based Force Sensors[J]. Sensors, 2017, 17(2): 229-240.